Supplementary Information

A Comprehensive Study on the Effect of Backbone Stereochemistry of a Cyclic Hexapeptide on Membrane Permeability and Microsomal Stability

Yuki Hosono,[a] Jumpei Morimoto,[*a] Shinsuke Sando[*a,b]

[a]*Department of Chemistry and Biotechnology, Graduate School of Engineering, The University of Tokyo, 7-3-1 Hongo, Bunkyo-ku, Tokyo 113-8656, Japan*

[b]*Department of Bioengineering, Graduate School of Engineering, The University of Tokyo, 7-3-1 Hongo, Bunkyo-ku, Tokyo 113-8656, Japan*

e-mail: jmorimoto@chembio.t.u-tokyo.ac.jp, ssando@chembio.t.u-tokyo.ac.jp

Table of contents

1. Abbreviations *3*

2. General remarks *3*

3. Synthesis *3*

3-1. Cyclic peptides CHP1–64 and a linear peptide LHP1 3

3-2. Library construction and synthesis of CHP19L, CHP37L, CHP61L, and CHP64L 5

4. Assay *6*

4-1. Measurement of membrane permeability by PAMPA 6

4-2. Measurement of 1,9-decadine–water distribution coefficients (Log$D_{dec/w}$) 7

4-3. Conformational analysis 7

4-4. Measurement of rat liver microsomal stability 8

4-5. Measurement of rat serum stability 9

5. Figures *10*

Fig. S1 Evaluation of correlations between membrane permeability and lipophilicity/conformational states. .. 10

Fig. S2 Speculated mechanisms of membrane permeability of CHP19, 37, 61 and 64 based on the conformational analysis. 11

Fig. S3 Measurement of metabolic stability in rat liver microsomes without NADPH. 12

Fig. S4 Conformational analysis of four diastereomers with the lowest metabolic stabilities (CHP40, 60, 64 and 59) and four diastereomers with the highest metabolic stabilities (CHP24, 1, 23 and 61). 13

Fig. S5 Evaluation of the correlations between metabolic stability and lipophilicity of CHP1–64. 14

Fig. S6 Measurement of stability of cyclic hexapeptide diastereomers in 50% rat serum 15

Fig. S7 UPLC chromatograms of purified compounds. 16

6. Table *22*

Table S1 MALDI-TOF MS analysis of CHP1–64 22

7. References *23*

1. Abbreviations

HPLC, high performance liquid chromatography; UPLC, ultra performance liquid chromatography; LC-MS, liquid chromatography-mass spectrometer; MALDI-TOF MS, matrix assisted laser desorption/ionization-time of flight mass spectrometry; CTC resin, 2-chlorotriryl chloride resin; DCM, dichloromethane; Fmoc, 9-fluorenylmethyloxycarbonyl; DIPEA, *N*,*N*-diisopropylethylamine; DMF, *N*,*N*-dimethylformamide; HATU, 1-[bis(dimethylamino)methylene]-1H-1,2,3-triazolo[4,5-b]pyridinium 3-oxide hexafluorophosphate; HOAt, 1-hydroxy-7-azabenzotriazole; HFIP, 1,1,1,3,3,3-hexafluoro-2-propanol; PyBOP, (benzotriazole-1-yloxy)trispyrrolidinophosphonium hexafluorophosphate; TFA, trifluoroacetic acid; ACN; acetonitrile; PyAOP, (7-Azabenzotriazol-1-yloxy)trispyrrolidinophosphonium hexafluorophosphate; PAMPA, parallel artificial membrane permeability assay; DMSO, *N*,*N*-dimethylformamide; PBS; phosphate-buffered saline; PVDF, polyvinylidene difluoride; NADPH、β-nicotinamide adenine dinucleotide phosphate reduced form; PB, phosphate buffer; EDTA, ethylenediaminetetraacetic acid

2. General remarks

Chemicals used in this study were purchased from commercial suppliers and used without further purification. Preparative HPLC was performed on a Prominence HPLC system (Shimadzu) with a $5C_{18}$-MS-II column (Nacalai tesque, 10 mm I.D.×150 mm, 34355-91). MALDI-TOF MS analysis was performed on autoflex speed (Bruker Daltonics) using DHB (Funakoshi) as matrix. LC-MS analysis and UPLC analysis was performed on a ACQUITYUPLC H-Class/SQD2 (Waters) using InertSustain AQ-C18 (GL Science, 2.1 I.D. x 50 mm). Automated peptide synthesis was performed using Syro I (Biotage).

3. Synthesis

3-1. Cyclic peptides CHP1–64 and a linear peptide LHP1

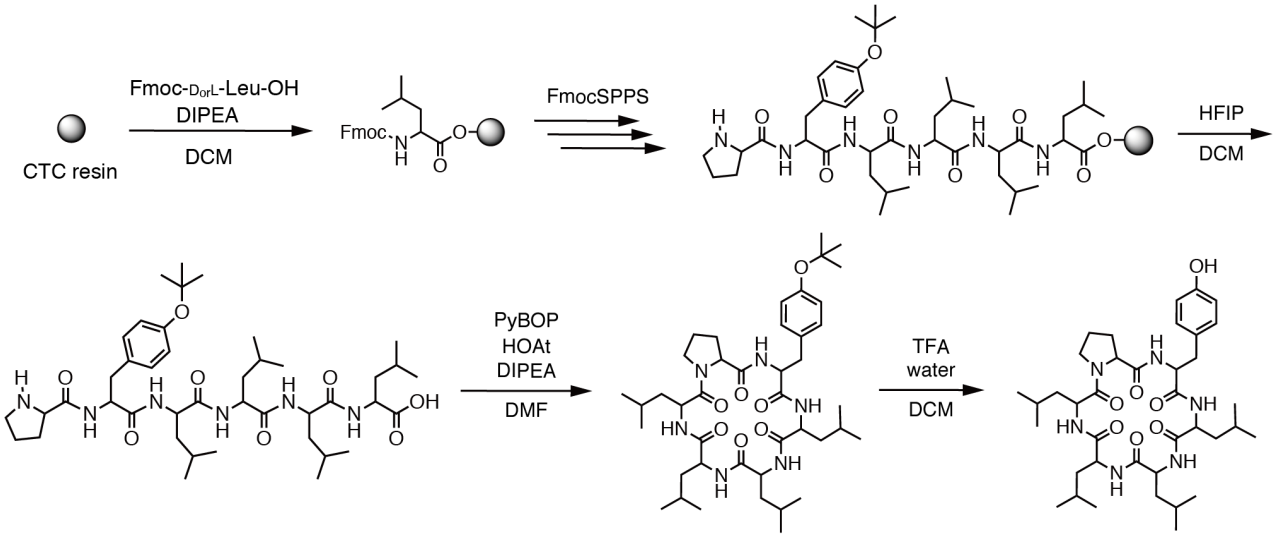

The peptide was synthesized on CTC resin (1.37 mmol/g). Resin (256 mg, 351 μmol) was swelled with DCM in a 12 mL fritted syringe with continuous shaking. Fmoc-L-Leu-OH (248 mg, 702 μmol, 2 equiv.) or Fmoc-D-Leu-OH (248 mg, 702 μmol, 2 equiv.) and DIPEA (244 μL, 1.40 mmol, 4 equiv.) were dissolved in 6 mL DCM and the solution was added to the resin. The resin was shaken overnight at room temperature. After the reaction, the resin was washed with DCM and 17:2:1 DCM:methanol:DIPEA three times each. The resin was applied to further peptide synthesis. 4 mg of the resin was transferred into syringes and the peptides were individually synthesized using an automated peptide synthesizer. Fmoc deprotection was performed by shaking the resin with 20% piperidine/DMF for 3 min; then shaking the resin with 20% piperidine/DMF for 12 min. The resin was washed with DMF six times. Coupling reaction was performed by shaking the resin with Fmoc-protected amino acid (4 equiv.), HATU (4 equiv.), and DIPEA (8 equiv.) in 600 μL of DMF for 2 h at room temperature. After the reaction, the resin was washed with DMF three times. The deprotection and coupling reaction were repeated until the N-terminal L-Pro or D-Pro residue. After the automated synthesis, the following synthetic procedures were manually performed. Fmoc group was removed by shaking the resin with 20% piperidine/DMF for 3 min. After washed with DMF three times, the resin was shaken with 20% piperidine/DMF for 12 min to complete deprotection and the resin was washed with DMF and DCM three times each. The precursor linear peptide was cleaved from the resin by shaking the resin with 30% HFIP/DCM for 15 min three times. The filtrate was collected in a 9 mL vial and the solvent was evaporated. The peptide was dissolved in 2 mL of DMF containing PyBOP (4.3 mg, 8.2 μmol, 1.5 equiv.) and HOAt (1.1 mg, 8.2 μmol, 1.5 equiv.). DIPEA (4.3 μL, 24.7 μmol, 4.5 equiv.) was added to the solution and the vial was shaken overnight at room temperature to perform cyclization of the peptide. After evaporation, the vial was shaken with 2 mL of 2.5% water/47.5% DCM/50% TFA for 1 h at room temperature to deprotect side chains. After evaporation, the peptide was dissolved in 50% ACN/water, purified by HPLC and lyophilized. After the lyophilization, the purified peptide was dissolved in DMSO yielding 10 mM **CHP1–64** solution based on the UV absorbance at 280 nm. **LHP1** was synthesized through the same procedure without cyclization. Purified **CHP1–64** and **LHP1** were analyzed by MALDI-TOF MS and UPLC (Fig. S7 and Table S1).

3-2. Library construction and synthesis of CHP19L, CHP37L, CHP61L, and CHP64L

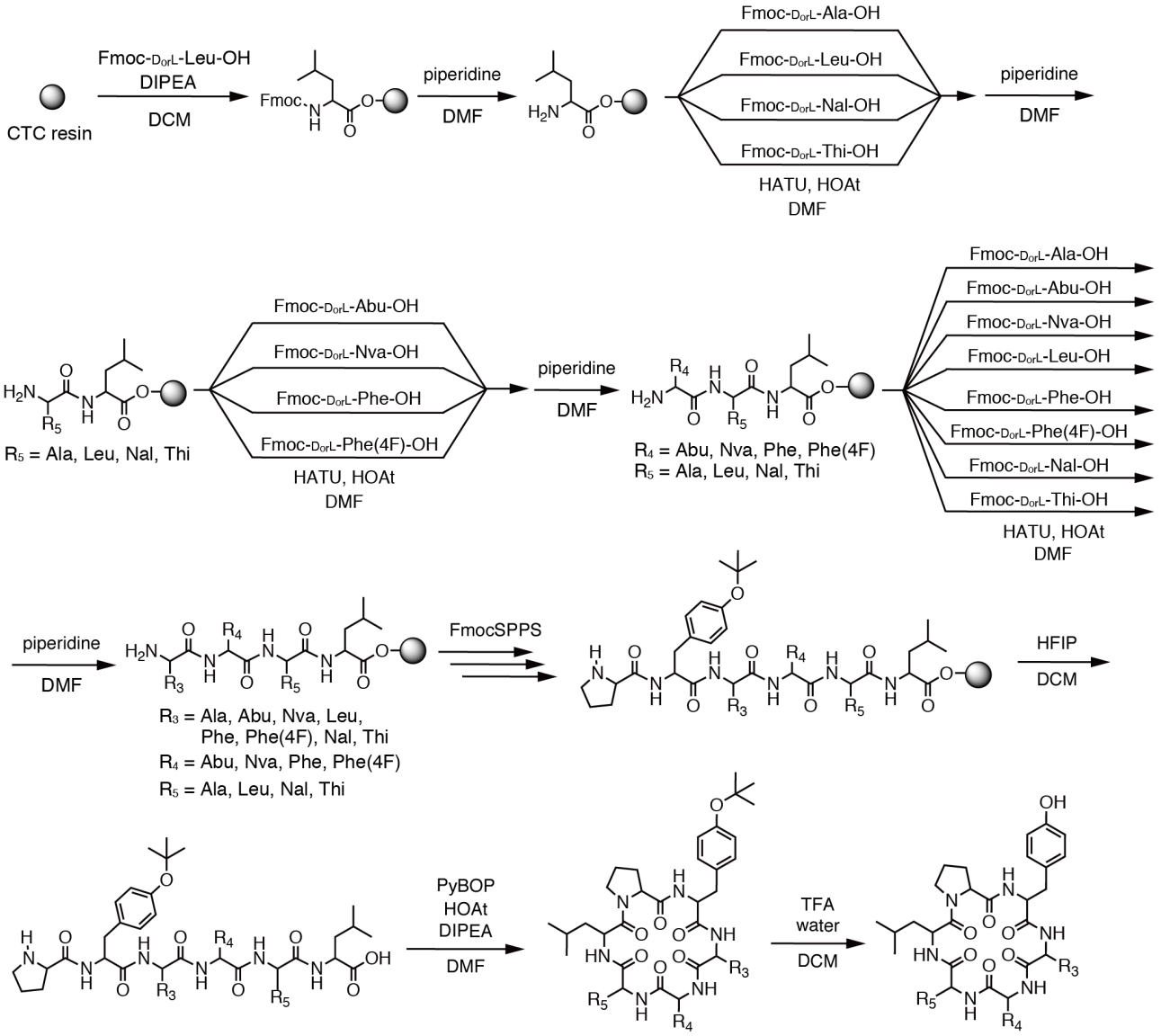

The peptides were synthesized on CTC resin (1.34 mmol/g). Resin (40 mg, 54 μmol) was swelled with DCM in a 6 mL fritted syringe with continuous shaking. Fmoc-L-Leu-OH (37.9 mg, 107 μmol, 2 equiv.) or Fmoc-D-Leu-OH (37.9 mg, 107 μmol, 2 equiv.) and DIPEA (37.4 μL, 214 μmol, 4 equiv.) were dissolved in 1 mL DCM and the solution was added to the resin. The resin was shaken for 2 h at room temperature. After the reaction, the resin was washed with DCM and 17:2:1 DCM:methanol:DIPEA three times each. Fmoc deprotection was performed by shaking the resin with 20% piperidine/DMF for 3 min. After washing the resin briefly with DMF, the resin was shaken with 20% piperidine/DMF for 12 min to complete deprotection and the resin was washed with DMF three times. The resin was split into four syringes and the subsequent coupling reaction was performed in each syringe by shaking the resin with Fmoc-DorL-Ala-OH (19.5 mg, 60 μmol, 4.5 equiv.), Fmoc-DorL-Leu-OH (21.2 mg, 60 μmol, 4.5 equiv.), Fmoc-DorL-Nal-OH (26.3 mg, 60 μmol, 4.5 equiv.), or Fmoc-DorL-Thi-OH (23.6 mg, 60 μmol, 4.5 equiv.), HATU (22.8 mg, 60 μmol, 4.5 equiv.), and DIPEA (20.9 μL 120 μmol, 9 equiv.) in 600 μL of DMF for 1 h at room temperature. After the reaction, the resin was washed with DMF

three times. The resin in the syringes was collected in a 6 mL syringe and Fmoc deprotection was performed with the procedures described above. After the Fmoc deprotection, the resin was again split into four syringes and subsequent coupling reaction was performed in each syringe by shaking the resin with Fmoc-D$_{or}$L-Abu-OH (19.5 mg, 60 μmol, 4.5 equiv.), Fmoc-D$_{or}$L-Nva-OH (20.3 mg, 60 μmol, 4.5 equiv.), Fmoc-D$_{or}$L-Phe-OH (23.2 mg, 60 μmol, 4.5 equiv.), or Fmoc-D$_{or}$L-Phe(4F)-OH (24.3 mg, 60 μmol, 4.5 equiv.), HATU (22.8 mg, 60 μmol, 4.5 equiv.), and DIPEA (20.9 μL 120 μmol, 9 equiv.) in 600 μL of DMF for 1 h at room temperature. After the reaction, the resin was washed with DMF three times. The resin in the syringes was collected in a 6 mL syringe, well mixed and split into eight syringes and the remaining peptide synthesis was performed in parallel on an automated peptide synthesizer. Fmoc deprotection was performed by shaking the resin with 20% piperidine/DMF for 3 min; then shaking the resin with 20% piperidine/DMF for 12 min. The resin was washed with DMF six times. Coupling reaction was performed by shaking the resin with Fmoc-protected amino acid (6 equiv.), HATU (6 equiv.), and DIPEA (12 equiv.) in 600 μL of DMF for 2 h at room temperature. After the reaction, the resin was washed with DMF three times. Above deprotection and coupling reaction were repeated until the N-terminal Pro or D-Pro residue. After the automated synthesis, the following synthetic procedures were manually performed. Fmoc group was removed by shaking the resin with 20% piperidine/DMF for 3 min. After washed with DMF three times, the resin was shaken with 20% piperidine/DMF for 12 min to complete deprotection and the resin was washed with DMF and DCM three times each. The precursor linear peptide was cleaved from the resin by shaking the resin with 20% HFIP/DCM for 15 min three times. The filtrate was collected in a 9 mL vial and evaporated. The peptide was dissolved in 2 mL of DMF containing PyAOP (5.3 mg, 10 μmol, 1.5 equiv.) and HOAt (1.3 mg, 10 μmol, 1.5 equiv.). DIPEA (5.3 μL, 30 μmol, 4.5 equiv.) was added to the solution and the vial was shaken overnight at room temperature to cyclize the peptide. After evaporation, the vial was shaken with 2 mL of 2.5% water/47.5% DCM/50% TFA for 1 h at room temperature to deprotect the Tyr residue. After evaporation, the peptide was dissolved in 50% ACN/water and lyophilized. The lyophilized peptides were dissolved in ACN/water and purified using a solid phase extraction column (ISOLUTE C18(EC), biotage). The eluate was lyophilized, and the purified peptides were dissolved in DMSO at a gross concentration of 20 mM based on the UV absorbance at 280 nm. Purified **CHP19L**, **CHP37L, CHP61L**, and **CHP64L** were analyzed by MALDI-TOF MS (the list of calculated and observed masses are attached as a csv file).

4. Assay

4-1. Measurement of membrane permeability by PAMPA

Membrane permeability across artificial membrane was measured using PAMPA according to the previously reported procedures[1] with minor modifications. The assay was conducted using MultiScreen-IP Filter Plate, 0.45 μm (Merck) and MultiScreen 96-well Transport Receiver Plate (Merck). 300 μL of 5% DMSO/PBS was added to each well of the acceptor plate. 5 μL of 1% lecithin from soybean (Alfa Aesar) in dodecane was carefully added on PVDF membrane of each well of the donor plate for preparing an artificial lipid membrane. 150 μL of compound solution was added to each well of the donor plate. Compound solution contained 2 μM of **CHP1–64** or 100 μM gross concentration of libraries in 5% DMSO/PBS. The donor plate was docked on the acceptor plate and the plates were incubated in a box containing a wet

paper towel at 25 ºC for 16 h. After incubation, the ratio of the concentrations of compounds in a donor well and an acceptor well was determined by LC-MS. By using the determined ratio, the effective permeability coefficient (P_e) of each compound was calculated using the following equation:

$$P_e = -\frac{ln[1-(V_A+V_D)/(V_A+R(t)\times V_D)]}{A\times(1/V_D+1/V_A)\times t}$$

Where:

A = filter area (0.3 cm^2)

V_D = donor well volume (0.15 mL)

V_A = acceptor well volume (0.30 mL)

t = incubation time (s)

$R(t)$ = ratio of LC-MS peak area in a donor well to that in an acceptor well at time t

For the measurements of **CHP1–64**, **CHP9** was used as an external standard. P_e of **CHP9** (0.9×10^{-6} cm/s) was separately determined by PAMPA and used as the external standard value.

4-2. Measurement of 1,9-decadine–water distribution coefficients (Log$D_{dec/w}$)

1,9-decadiene–water distribution coefficients (Log$D_{dec/w}$) was measured according to the previously reported procedures[2] with minor modifications. 1,9-Decadiene was saturated with water by shaking with an equal volume of PBS (pH 7.4) overnight. 0.5 μL of 400 μM **CHP1–64** in DMSO was added to PCR tubes. 50 μL of water-saturated 1,9-decadiene and the same volume of PBS were added to yield a final concentration per compound of 2 μM. The tubes were vortexed over 1 h at room temperature. The emulsions were centrifuged at 7,000 rpm until the emulsions completely separated. 40 μL of each layer was carefully transferred to 1.5 mL tubes. The organic layer was recovered and evaporated using Savant SpeedVac (Thermo) at 60 ºC, and then 200 μL of 50% ACN/PBS was added and vortexed to dissolve compounds. The aqueous layer was recovered and 110 μL of PBS and 150 μL ACN were added to yield the compound solution in 50% ACN/PBS. Each solution was analyzed by LC-MS. Log$D_{dec/w}$ was calculated using the following equations:

$$\mathrm{Log}D_{\mathrm{dec/w}} = \log R(t)$$

Where:

$R(t)$ = ratio of LC-MS peak area in an organic layer to that in a PBS layer at time t

CHP9 was used as an external standard (Log$D_{dec/w}$ = −1.34).

4-3. Conformational analysis

Conformations were generated by OpenEye Scientific's OMEGA program in macrocyclic mode[3] with dielectric constants of 1.9 and 74.4 for mimicking lipophilic and hydrophilic environments, respectively. Average IMHBs were calculated using conformers within 10 kcal/mol from the lowest energy. The IMHB pattern was calculated with the donor–acceptor atomic distance below 0.35 nm and angle below 30º.[4] Each IMHB was weighted by the occupancy of the given conformation (r_i) which was calculated with a relative energy to the lowest energy conformers using following equations.

$$Average\ IMHB = \sum_i (IMHB_i \times r_i)$$

$$r_i = \frac{\exp\left(-\frac{\Delta E_{i0}}{RT}\right)}{\sum_i^N \exp\left(-\frac{\Delta E_{i0}}{RT}\right)}$$

Where:

$IMHB_i$ = the number of IMHB in conformer i

N = the number of conformers within 10 kcal/mol from the lowest energy

ΔE_{i0} = relative energy of conformer i to the lowest energy

R = the gas constant

T = temperature (310 K)

In the conformational analysis for speculating the permeation mechanisms of **CHP19**, **CHP37**, **CHP61**, and **CHP64**, the relative abundance of conformers was calculated using conformers within 2 kcal/mol from the lowest energy.

4-4. Measurement of rat liver microsomal stability

Metabolic stability in rat liver microsomes was measured according to the previously reported procedures[5] with minor modifications. 5 μL for individual and 10 μL for library of 10 mM NADPH (Oriental Yeast Co., Ltd.) in 0.1 M PB (pH 7.4) and the same volume of 10 μM **CHP1–64** in 0.1 M PB (pH 7.4) containing 1% DMSO or a library containing peptides of 200 μM gross concentration in 0.1 M PB (pH 7.4) containing 10% DMSO were added into a PCR tube. Pre-mixed solution which contained 0.25 mg/mL rat liver microsomes (Sekisui XenoTech, LLC) in clearance buffer (0.1 M PB (pH 7.4) containing 1.25 mM EDTA) was incubated for 5 min at 37 ºC. After the incubation, 40 μL for individual and 80 μL for library of pre-mixed solution was added to the PCR tube which had been preincubated for 5 min at 37 ºC and the PCR tube was incubated at 37 ºC for 30 min. A fraction of the solution was immediately transferred to another PCR tube which contained 5 times the volume of ice-cold ACN as a control. At time 30 min, another fraction of the solution was transferred to another PCR tube which contained 5 times the volume of ice-cold ACN. The solution containing **CHP1–64** was filtered and the filtered solution was analyzed by LC-MS to determine the ratio of the concentration of the intact compound at 0 and 30 min. The solution containing libraries was centrifuged at 7,000 rpm for 10 min and the supernatant was analyzed by LC-MS. For stability assay without NADPH, 20 μL of 5 μM compounds in 0.1 M PB (pH 7.4) containing 0.5% DMSO were added to a PCR tube and preincubated for 5 min at 37 ºC. Then, 80 μL of pre-mixed solution which had been preincubated for 5 min at 37 ºC. Following procedure was the same as that for **CHP1–64** described above. *In vitro* intrinsic clearance (CL_{int}) of each compound was calculated using the following equations:

$$t_{\frac{1}{2}} = \frac{t}{\log_{\frac{1}{2}} R(t)}$$

$$CL_{int} = \frac{LN(2)}{MS \times t_{\frac{1}{2}}} \times 1000$$

$$\%Intact\ Peptide\ = R(t) \times 100$$

Where:

$t_{1/2}$ = half-life of the compound (min)

R(t) = ratio of LC-MS peak area at 30 min to that at 0 min

MS = concentration of rat liver microsomal proteins (0.2 mg/mL)

For the measurements of **CHP1–64**, **CHP9** was used as an external standard. A previously reported value (243 μL/min/mg) was used for the external standard CL_{int} value of **CHP9**.[5]

4-5. Measurement of rat serum stability

Serum stability was measured using rat serum (Sigma-Aldrich). 7 μL of 10 μM **CHP1–64** in PBS (pH 7.4) containing 1% DMSO and 28 μL of PBS (pH 7.4) were added to a PCR tube and incubated for 5 min at 37 ºC before the assay. 35 μL of rat serum which had been incubated for 5 min at 37 ºC were added to the PCR tube and incubated for 1 hour at 37 ºC. As a control, 30 μL of the solution was immediately transferred to another PCR tube which contained 150 μL of ice-cold ACN as a control. At time 1 h, 30 μL of the solution was transferred to another PCR tube which contained 150 μL of ice-cold ACN, and the tube was mixed vigorously. The solution was centrifuged at 7,000 rpm for 10 min. The supernatant was analyzed by LC-MS to determine the ratio of the concentration of the intact compound at 0 and 30 min. A linear hexapeptide named **LHP1** was included as a control to assure the proteolytic activity of the rat serum. Stability in rat serum was calculated using the following equation:

$$\%Intact\ Peptide\ = R(t) \times 100$$

Where:

R(t) = ratio of LC-MS peak area at 30 min to that at 0 min

5. Figures

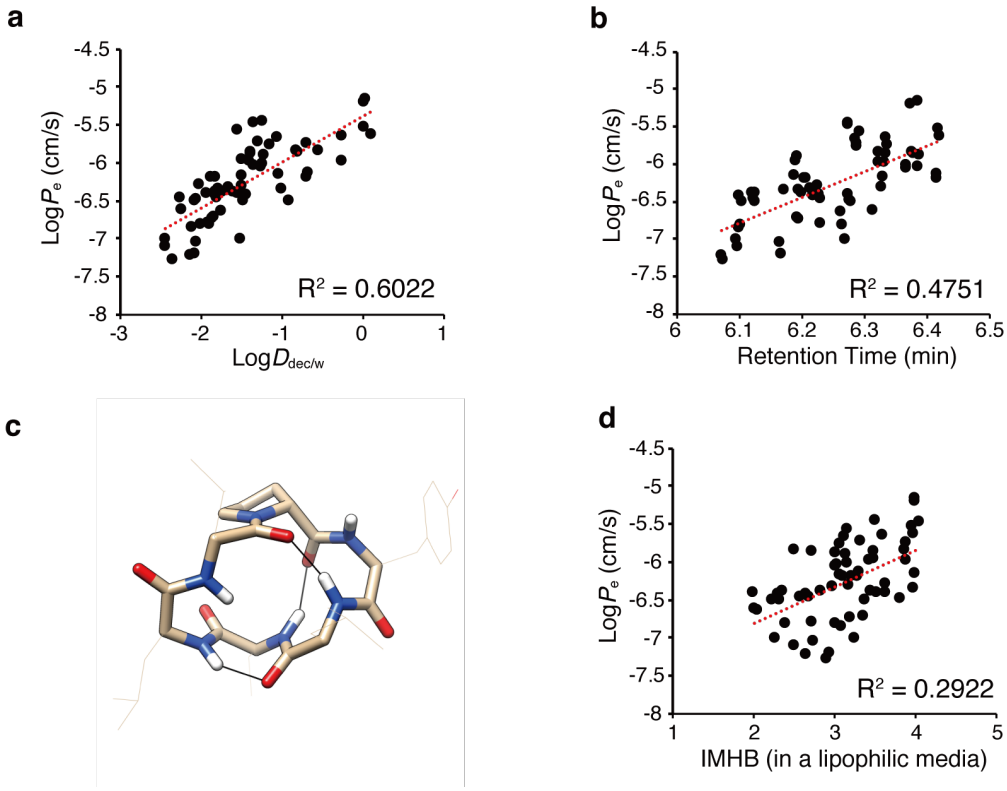

Fig. S1 Evaluation of correlations between membrane permeability and lipophilicity/conformational states.

The correlations between membrane permeability measured by PAMPA and (a) Log$D_{dec/w}$ and (b) UPLC retention time. (c) The lowest energy conformer of **CHP9** determined by MM calculations. (d) The correlations between membrane permeability measured by PAMPA and the average number of IMHB of conformers within 10 kcal/mol from the lowest energy calculated with a dielectric constant of 1.9.

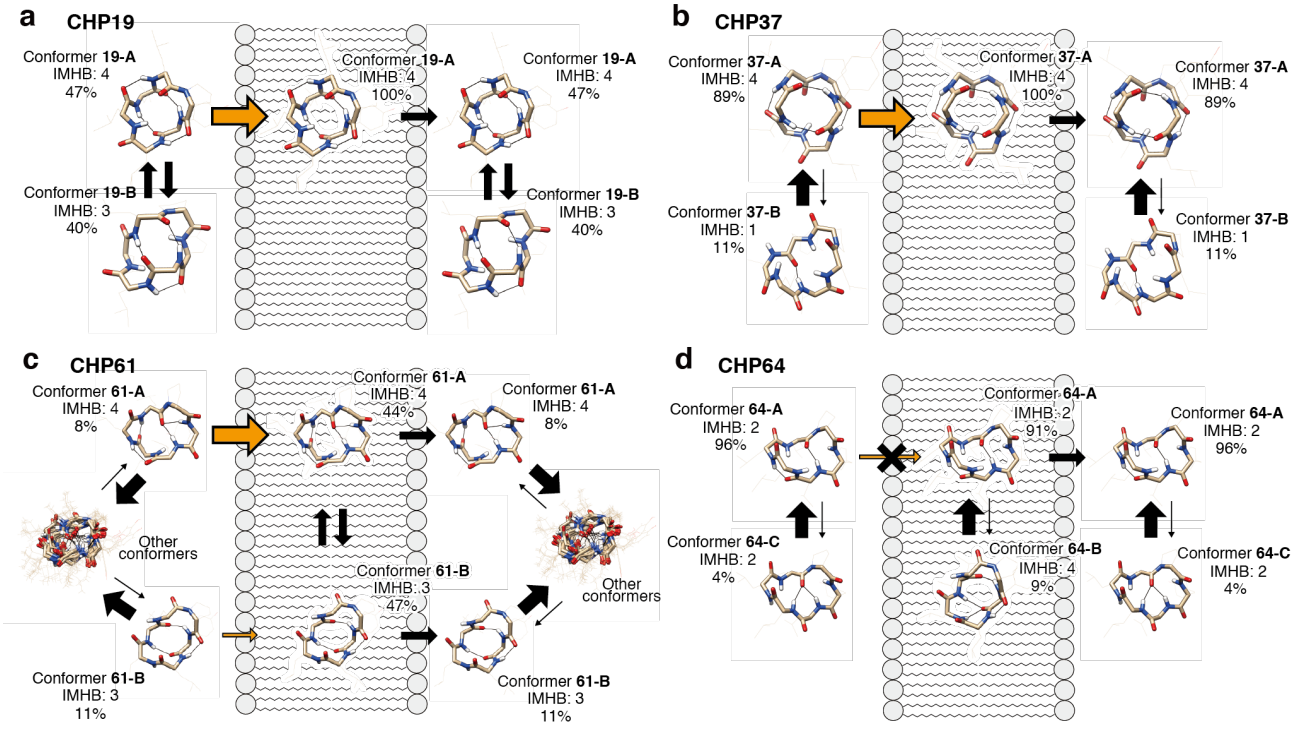

Fig. S2 Speculated mechanisms of membrane permeability of CHP19, 37, 61 and 64 based on the conformational analysis. Major conformations of each peptide in water and hexane obtained from MM calculations are shown and a speculated membrane permeation mechanism based on the conformations is illustrated for (a) **CHP19**, (b) **CHP37**, (c) **CHP61**, and (d) **CHP64**.

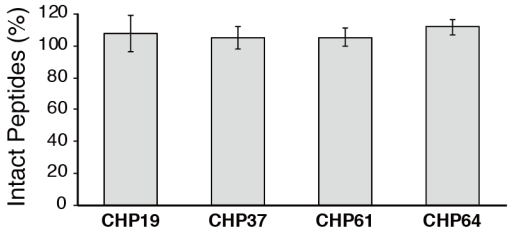

Fig. S3 Measurement of metabolic stability in rat liver microsomes without NADPH.

Metabolic stability of **CHP19**, **37**, **61**, and **64** in rat liver microsomes without NADPH. Each bar represents the mean value and the standard deviations from experiments carried out in quadruplicate.

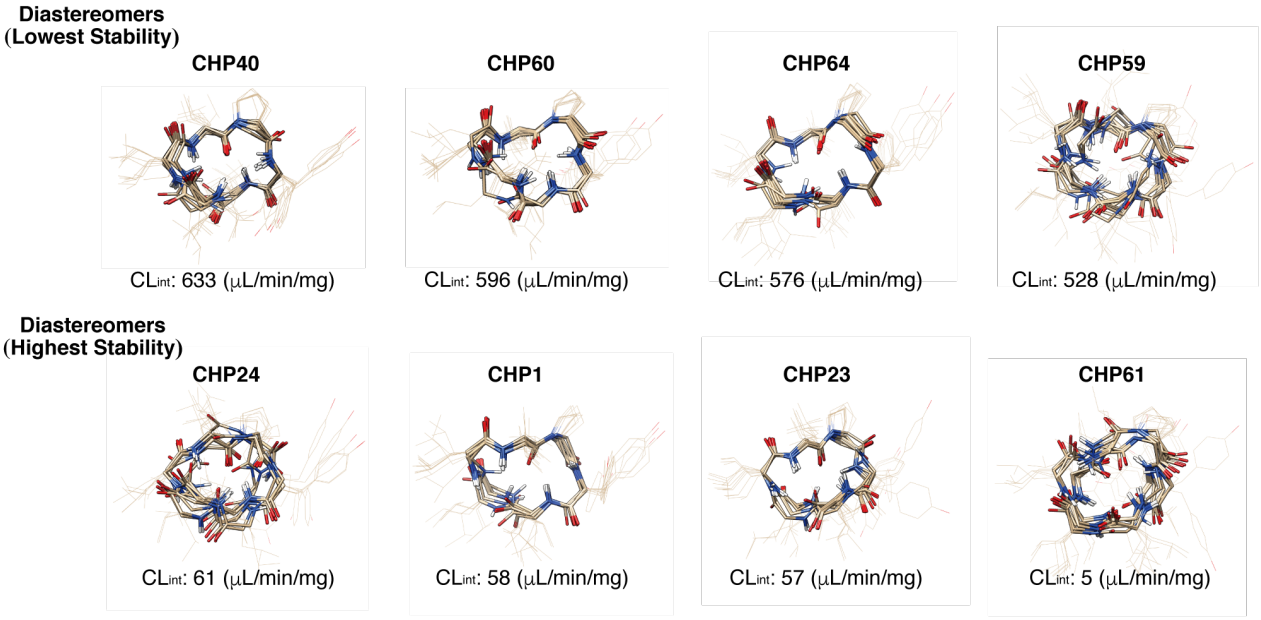

Fig. S4 Conformational analysis of four diastereomers with the lowest metabolic stabilities (CHP40, 60, 64 and 59) and four diastereomers with the highest metabolic stabilities (CHP24, 1, 23 and 61).

Conformers were generated by MM calculations and 10 conformers with the lowest energies were superposed for each diastereomer.

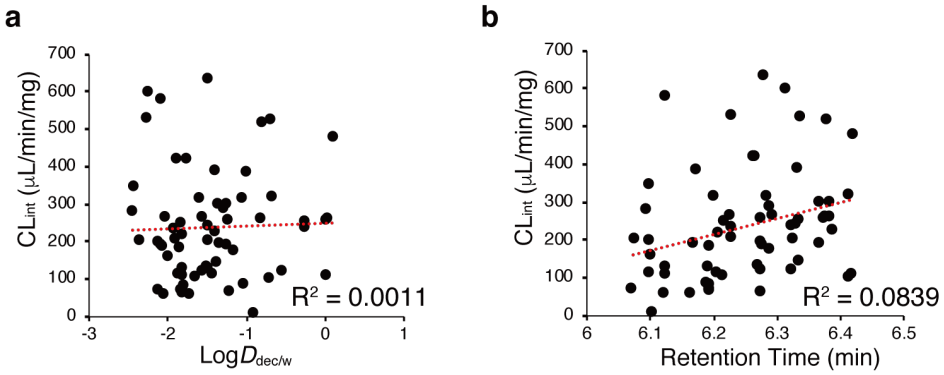

Fig. S5 Evaluation of the correlations between metabolic stability and lipophilicity of CHP1–64.

The correlations between the rat liver microsomal stability and (a) Log$D_{dec/w}$ and (b) UPLC retention time are plotted.

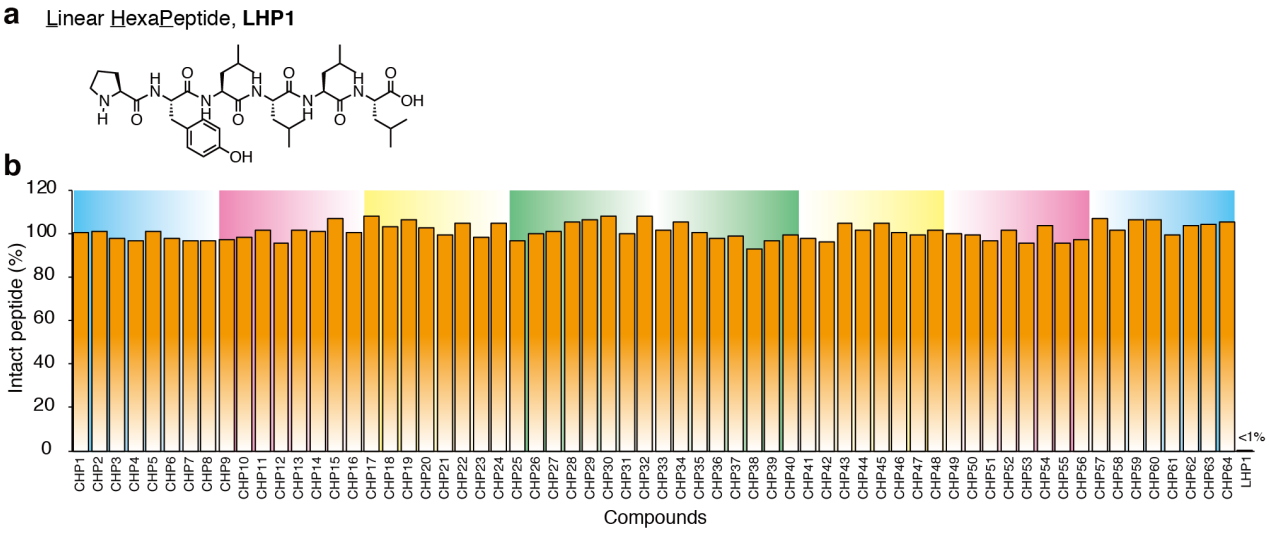

Fig. S6 Measurement of stability of cyclic hexapeptide diastereomers in 50% rat serum

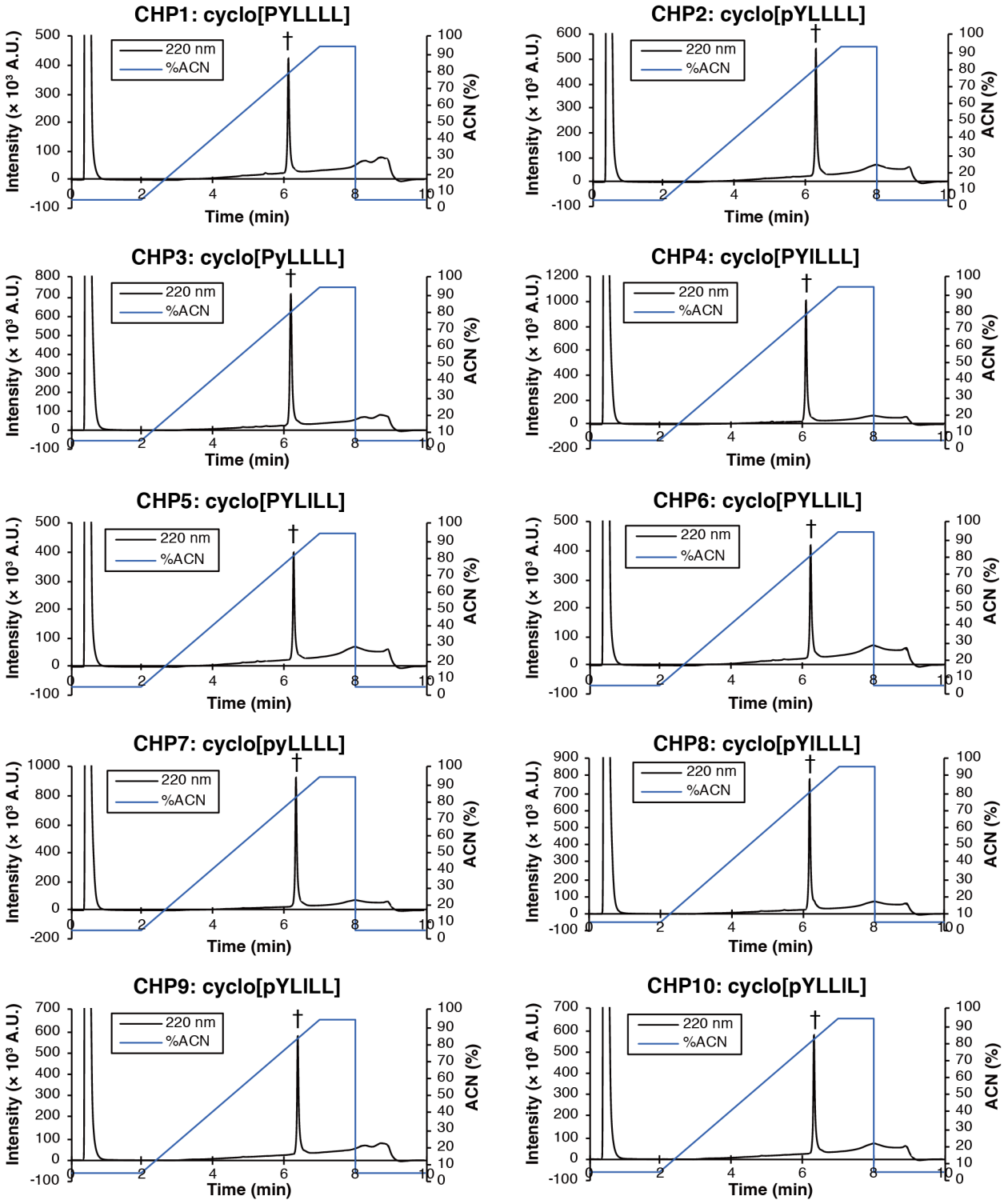

Fig. S7 UPLC chromatograms of purified compounds.

UV chromatograms of **CHP1–64** and **LHP1** after purification measured on UPLC. † denotes the fraction containing desired product. Products were monitored at 220 nm. Sequences are described after the name of each compound. The UPLC analysis was performed using a linear gradient of water containing 0.01% formic acid and ACN containing 0.01% formic acid. Blue line denotes the percentage of ACN. The peak appeared at 0–1 min is derived from DMSO.

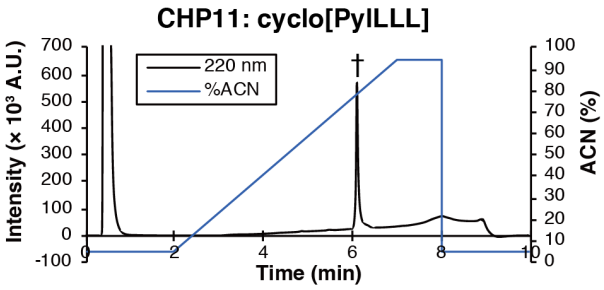
CHP11: cyclo[PylLLL]
220 nm
%ACN
†
Intensity (× 10³ A.U.)
ACN (%)
Time (min)

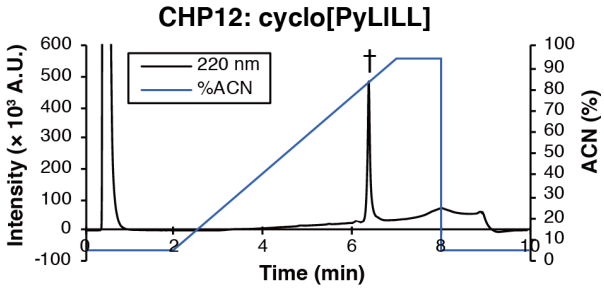
CHP12: cyclo[PyLlLL]
220 nm
%ACN
†
Intensity (× 10³ A.U.)
ACN (%)
Time (min)

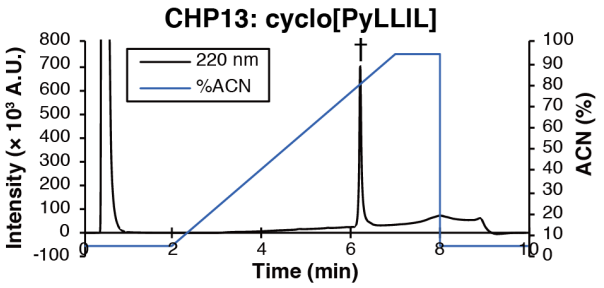
CHP13: cyclo[PyLLlL]
220 nm
%ACN
†
Intensity (× 10³ A.U.)
ACN (%)
Time (min)

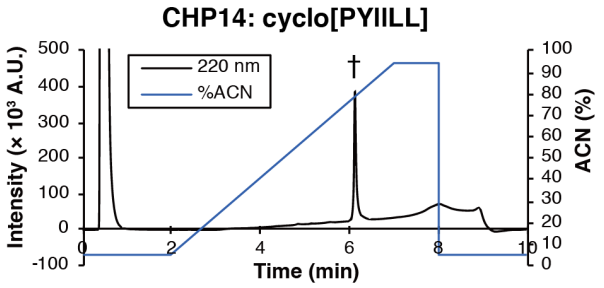
CHP14: cyclo[PYlLL]
220 nm
%ACN
†
Intensity (× 10³ A.U.)
ACN (%)
Time (min)

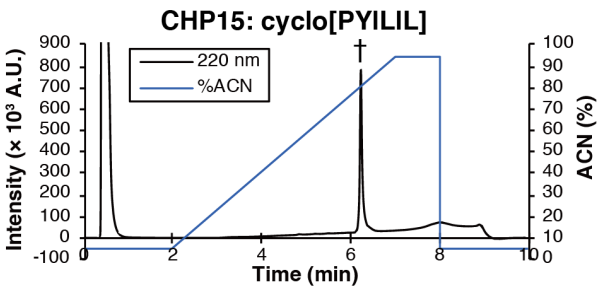
CHP15: cyclo[PYlLlL]
220 nm
%ACN
†
Intensity (× 10³ A.U.)
ACN (%)
Time (min)

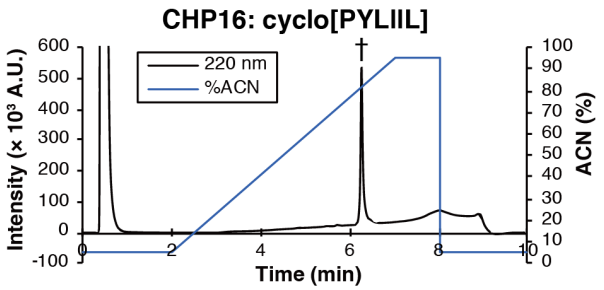
CHP16: cyclo[PYLlIL]
220 nm
%ACN
†
Intensity (× 10³ A.U.)
ACN (%)
Time (min)

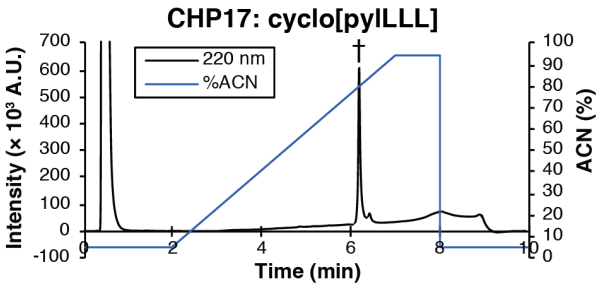
CHP17: cyclo[pylLLL]
220 nm
%ACN
†
Intensity (× 10³ A.U.)
ACN (%)
Time (min)

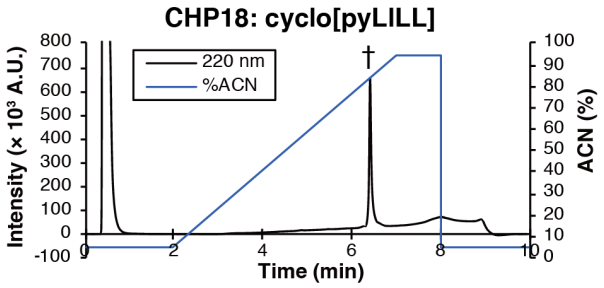
CHP18: cyclo[pyLlLL]
220 nm
%ACN
†
Intensity (× 10³ A.U.)
ACN (%)
Time (min)

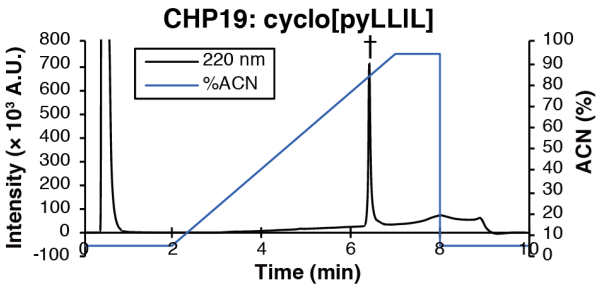
CHP19: cyclo[pyLLlL]
220 nm
%ACN
†
Intensity (× 10³ A.U.)
ACN (%)
Time (min)

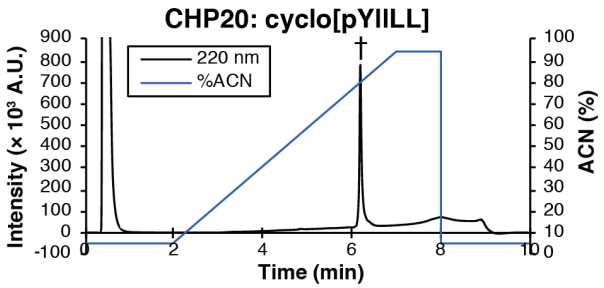
CHP20: cyclo[pYlLL]
220 nm
%ACN
†
Intensity (× 10³ A.U.)
ACN (%)
Time (min)

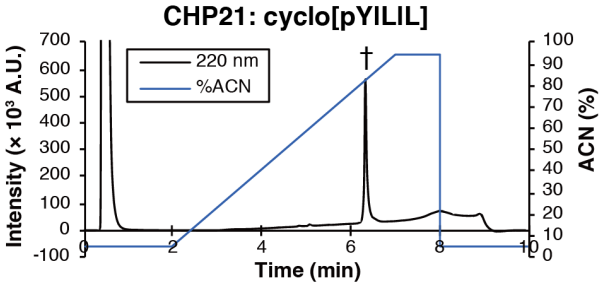
CHP21: cyclo[pYlLlL]
220 nm
%ACN
†
Intensity (× 10³ A.U.)
ACN (%)
Time (min)

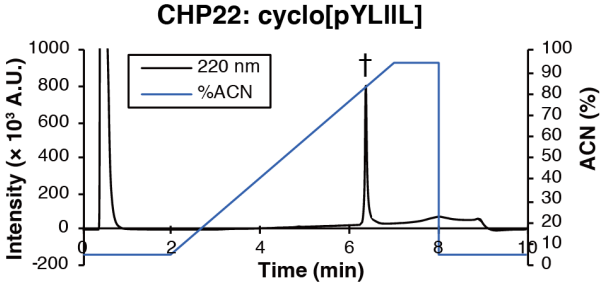
CHP22: cyclo[pYLlIL]
220 nm
%ACN
†
Intensity (× 10³ A.U.)
ACN (%)
Time (min)

Continued.

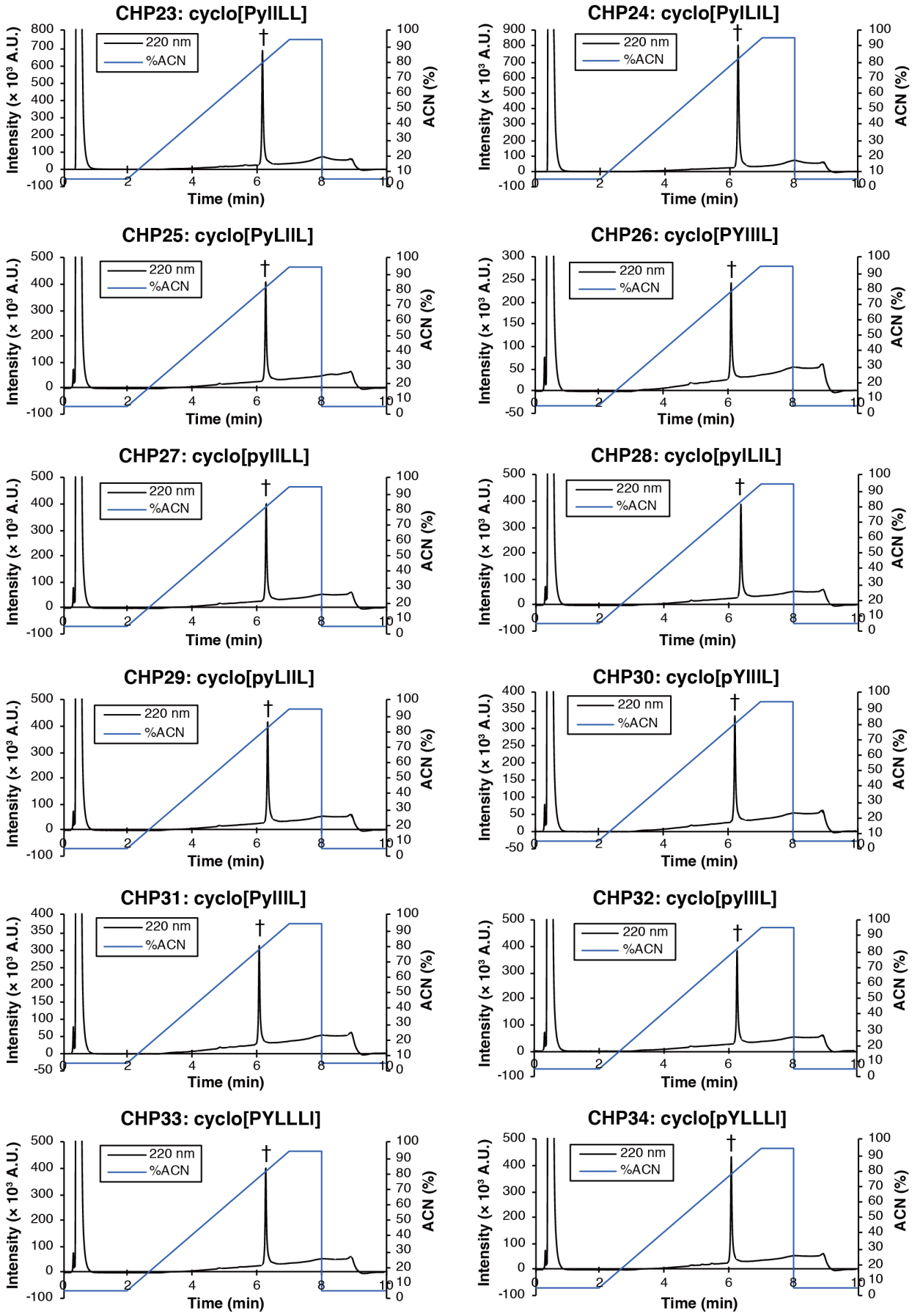
CHP23: cyclo[PyIILL]
CHP24: cyclo[PyILIL]
CHP25: cyclo[PyLIIL]
CHP26: cyclo[PYIIIL]
CHP27: cyclo[pyIILL]
CHP28: cyclo[pyILIL]
CHP29: cyclo[pyLIIL]
CHP30: cyclo[pYIIIL]
CHP31: cyclo[PyIIIL]
CHP32: cyclo[pyIIIL]
CHP33: cyclo[PYLLLI]
CHP34: cyclo[pYLLLI]
220 nm
%ACN
Intensity (× 10³ A.U.)
ACN (%)
Time (min)

Continued.

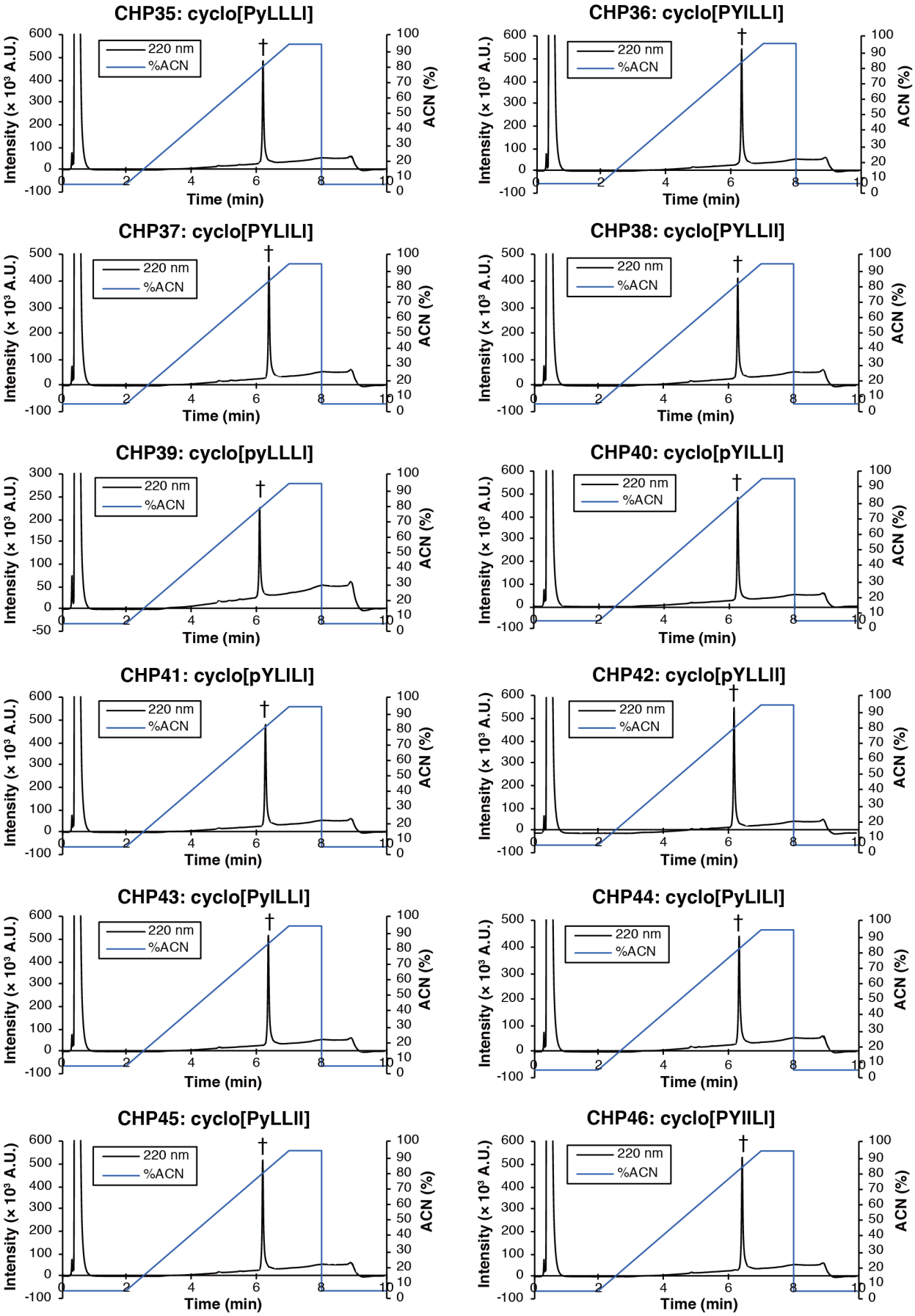
CHP35: cyclo[PyLLLl]
CHP36: cyclo[PYlLLl]
CHP37: cyclo[PYLlLl]
CHP38: cyclo[PYLLll]
CHP39: cyclo[pyLLLl]
CHP40: cyclo[pYlLLl]
CHP41: cyclo[pYLlLl]
CHP42: cyclo[pYLLll]
CHP43: cyclo[PylLLl]
CHP44: cyclo[PyLlLl]
CHP45: cyclo[PyLLll]
CHP46: cyclo[PYllLl]
220 nm
%ACN
Intensity (× 10³ A.U.)
ACN (%)
Time (min)

Continued.

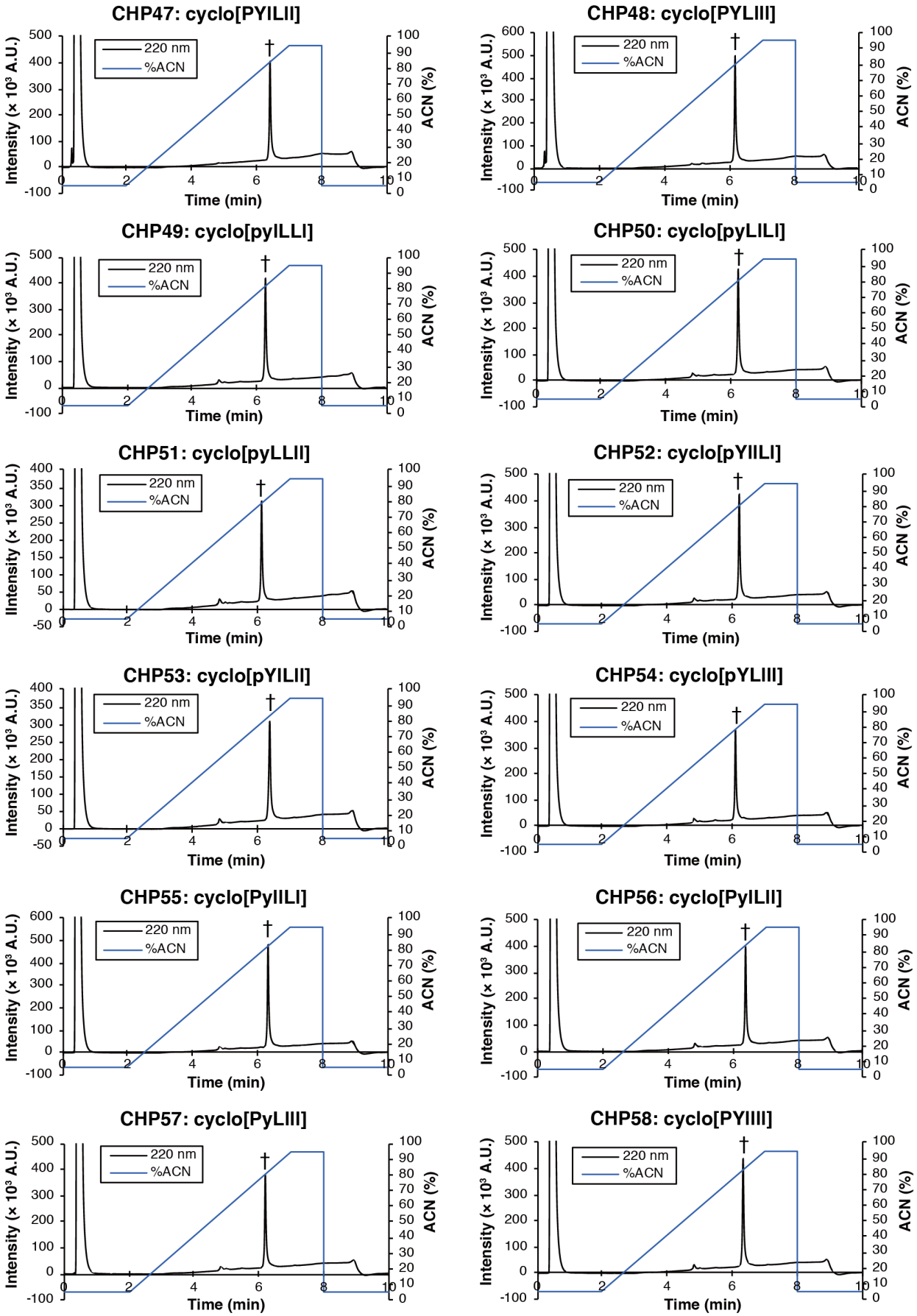
CHP47: cyclo[PYILll]
CHP48: cyclo[PYLlll]
CHP49: cyclo[pylLLl]
CHP50: cyclo[pyLlLl]
CHP51: cyclo[pyLLll]
CHP52: cyclo[pYllLl]
CHP53: cyclo[pYILll]
CHP54: cyclo[pYLlll]
CHP55: cyclo[PylILl]
CHP56: cyclo[PylLll]
CHP57: cyclo[PyLlll]
CHP58: cyclo[PYllll]
220 nm
%ACN
Intensity (× 10³ A.U.)
ACN (%)
Time (min)

Continued.

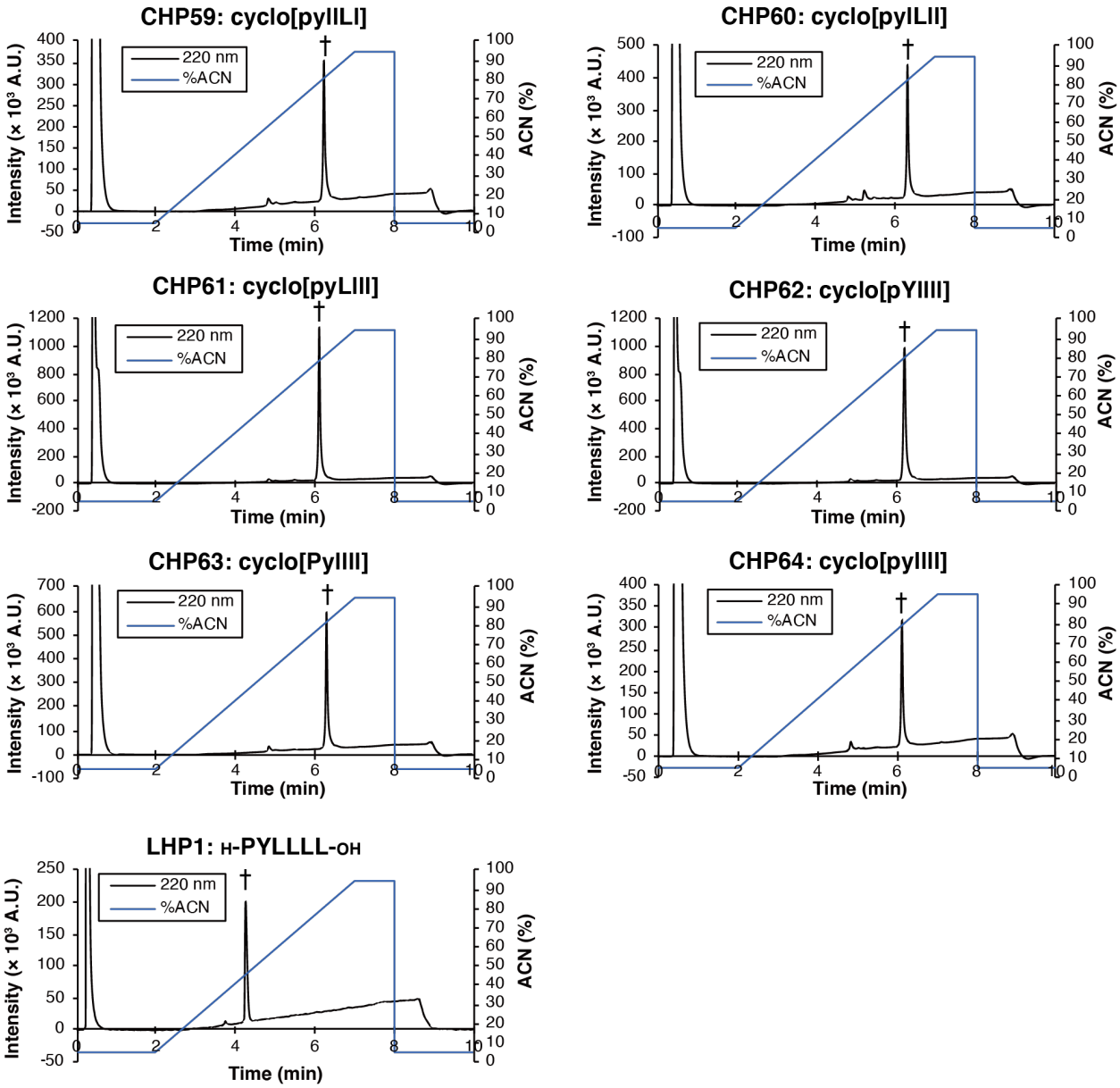
CHP59: cyclo[pyllLl]
CHP60: cyclo[pylLll]
CHP61: cyclo[pyLlll]
CHP62: cyclo[pYllll]
CHP63: cyclo[Pyllll]
CHP64: cyclo[pyllll]
LHP1: H-PYLLLL-OH
220 nm
%ACN
Intensity (× 10³ A.U.)
ACN (%)
Time (min)

Continued.

6. Table

Table S1 MALDI-TOF MS analysis of CHP1–64

		Calcd.		Obsd.
Name	sequence	Mw	$[M+H]^+$	$[M+H]^+$
CHP1	cyclo[PYLLLL]	712.93	713.46	713.27
CHP2	cyclo[pYLLLL]	712.93	713.46	713.34
CHP3	cyclo[PyLLLL]	712.93	713.46	713.38
CHP4	cyclo[PYlLLL]	712.93	713.46	713.38
CHP5	cyclo[PYLlLL]	712.93	713.46	713.28
CHP6	cyclo[PYLLlL]	712.93	713.46	713.43
CHP7	cyclo[pyLLLL]	712.93	713.46	713.45
CHP8	cyclo[pYlLLL]	712.93	713.46	713.52
CHP9	cyclo[pYLlLL]	712.93	713.46	713.31
CHP10	cyclo[pYLLlL]	712.93	713.46	713.35
CHP11	cyclo[PylLLL]	712.93	713.46	713.40
CHP12	cyclo[PyLlLL]	712.93	713.46	713.43
CHP13	cyclo[PyLLlL]	712.93	713.46	713.44
CHP14	cyclo[PYllLL]	712.93	713.46	713.47
CHP15	cyclo[PYlLlL]	712.93	713.46	713.49
CHP16	cyclo[PYLllL]	712.93	713.46	713.53
CHP17	cyclo[pylLLL]	712.93	713.46	713.30
CHP18	cyclo[pyLlLL]	712.93	713.46	713.31
CHP19	cyclo[pyLLlL]	712.93	713.46	713.35
CHP20	cyclo[pYllLL]	712.93	713.46	713.39
CHP21	cyclo[pYlLlL]	712.93	713.46	713.43
CHP22	cyclo[pYLllL]	712.93	713.46	713.46
CHP23	cyclo[PyllLL]	712.93	713.46	713.50
CHP24	cyclo[PylLlL]	712.93	713.46	713.54
CHP25	cyclo[PyLllL]	712.93	713.46	713.29
CHP26	cyclo[PYlllL]	712.93	713.46	713.32
CHP27	cyclo[pyllLL]	712.93	713.46	713.36
CHP28	cyclo[pylLlL]	712.93	713.46	713.43
CHP29	cyclo[pyLllL]	712.93	713.46	713.44
CHP30	cyclo[pYlllL]	712.93	713.46	713.48
CHP31	cyclo[PylllL]	712.93	713.46	713.52
CHP32	cyclo[pylllL]	712.93	713.46	713.55
CHP33	cyclo[PYLLLl]	712.93	713.46	713.27
CHP34	cyclo[pYLLLl]	712.93	713.46	713.30
CHP35	cyclo[PyLLLl]	712.93	713.46	713.34
CHP36	cyclo[PYlLLl]	712.93	713.46	713.37
CHP37	cyclo[PYLlLl]	712.93	713.46	713.43
CHP38	cyclo[PYLLll]	712.93	713.46	713.47
CHP39	cyclo[pyLLLl]	712.93	713.46	713.52
CHP40	cyclo[pYlLLl]	712.93	713.46	713.56
CHP41	cyclo[pYLlLl]	712.93	713.46	713.27
CHP42	cyclo[pYLLll]	712.93	713.46	713.32
CHP43	cyclo[PylLLl]	712.93	713.46	713.35
CHP44	cyclo[PyLlLl]	712.93	713.46	713.39
CHP45	cyclo[PyLLll]	712.93	713.46	713.45
CHP46	cyclo[PYllLl]	712.93	713.46	713.49
CHP47	cyclo[PYlLll]	712.93	713.46	713.53
CHP48	cyclo[PYLlll]	712.93	713.46	713.58
CHP49	cyclo[pylLLl]	712.93	713.46	713.30
CHP50	cyclo[pyLlLl]	712.93	713.46	713.35
CHP51	cyclo[pyLLll]	712.93	713.46	713.37
CHP52	cyclo[pYllLl]	712.93	713.46	713.44
CHP53	cyclo[pYlLll]	712.93	713.46	713.47
CHP54	cyclo[pYLlll]	712.93	713.46	713.50
CHP55	cyclo[PyllLl]	712.93	713.46	713.55
CHP56	cyclo[PylLll]	712.93	713.46	713.57
CHP57	cyclo[PyLlll]	712.93	713.46	713.32
CHP58	cyclo[PYllll]	712.93	713.46	713.37
CHP59	cyclo[pyllLl]	712.93	713.46	713.40
CHP60	cyclo[pylLll]	712.93	713.46	713.45
CHP61	cyclo[pyLlll]	712.93	713.46	713.49
CHP62	cyclo[pYllll]	712.93	713.46	713.52
CHP63	cyclo[Pyllll]	712.93	713.46	713.56
CHP64	cyclo[pyllll]	712.93	713.46	713.59
LHP1	H-PYLLLL-OH	730.95	731.47	731.76

7. References

1 W. M. Hewitt, S. S. F. Leung, C. R. Pye, A. R. Ponkey, M. Bednarek, M. P. Jacobson and R. S. Lokey, *J. Am. Chem. Soc.*, 2015, **137**, 715–721.

2 M. R. Naylor, A. M. Ly, M. J. Handford, D. P. Ramos, C. R. Pye, A. Furukawa, V. G. Klein, R. P. Noland, Q. Edmondson, A. C. Turmon, W. M. Hewitt, J. Schwochert, C. E. Townsend, C. N. Kelly, M. J. Blanco and R. S. Lokey, *J. Med. Chem.*, 2018, **61**, 11169–11182.

3 P. C. D. Hawkins, A. G. Skillman, G. L. Warren, B. A. Ellingson and M. T. Stahl, *J. Chem. Inf. Model.*, 2010, **50**, 572–584.

4 S. Ono, M. R. Naylor, C. E. Townsend, C. Okumura, O. Okada and R. S. Lokey, *J. Chem. Inf. Model.*, 2019, **59**, 2952–2963.

5 T. R. White, C. M. Renzelman, A. C. Rand, T. Rezai, C. M. McEwen, V. M. Gelev, R. A. Turner, R. G. Linington, S. S. F. Leung, A. S. Kalgutkar, J. N. Bauman, Y. Zhang, S. Liras, D. A. Price, A. M. Mathiowetz, M. P. Jacobson and R. S. Lokey, *Nat. Chem. Biol.*, 2011, **7**, 810–817.